Journal of Physiology (1993), **472**, *pp.* 665–688
With 13 *figures*
Printed in Great Britain

EXOCYTOSIS ELICITED BY ACTION POTENTIALS AND VOLTAGE-CLAMP CALCIUM CURRENTS IN INDIVIDUAL MOUSE PANCREATIC B-CELLS

BY C. ÄMMÄLÄ, L. ELIASSON, K. BOKVIST, O. LARSSON, F. M. ASHCROFT* AND P. RORSMAN†

From the Department of Medical Biophysics, Gothenburg University, Medicinaregatan 11, S-413 90 Gothenburg, Sweden

(*Received 22 January 1993*)

SUMMARY

1. Measurements of membrane capacitance, as an indicator of exocytosis, and intracellular Ca^{2+} concentration ($[Ca^{2+}]_i$) were used to determine the Ca^{2+} dependence of secretion in single pancreatic B-cells.

2. Exocytosis was dependent on a rise in $[Ca^{2+}]_i$ and could be evoked by activation of voltage-dependent Ca^{2+} currents. The threshold for depolarization-induced release was 0·5 μM $[Ca^{2+}]_i$. Once the $[Ca^{2+}]_i$ threshold was exceeded, exocytosis was rapidly (< 50 ms) initiated. When *individual* pulses were applied, exocytosis stopped immediately upon repolarization and the Ca^{2+} channels closed, although $[Ca^{2+}]_i$ remained elevated for several seconds.

3. During *repetitive* stimulation (1 Hz), when $[Ca^{2+}]_i$ attained micromolar levels, exocytosis also took place during the interpulse intervals albeit at a slower rate than during the depolarizations.

4. Exocytosis could be initiated by simulated action potentials. Whereas a single action potential only produced a small capacitance increase, and in some cells even failed to stimulate release, larger and more consistent responses were obtained with $\geqslant$ four action potentials.

5. Comparison of the rates of exocytosis measured in response to depolarization, mobilization of Ca^{2+} from intracellular stores or infusion of Ca^{2+} through the patch pipette suggests that $[Ca^{2+}]_i$ at the secretory sites attains a concentration of several micromolar. This is much higher than the average $[Ca^{2+}]_i$ detected by microfluorimetry suggesting the existence of steep spatial gradients of $[Ca^{2+}]_i$ within the B-cell.

6. Inclusion of inhibitors of Ca^{2+}/calmodulin-dependent protein kinase II in the intracellular solution reduced the depolarization-induced exocytotic responses suggesting this enzyme may be involved in the coupling between elevation of $[Ca^{2+}]_i$ to stimulation of the secretory machinery.

7. The size of the unitary exocytotic event was 2 fF, corresponding to a secretory granule diameter of 250 nm.

* Permanent address: University Laboratory of Physiology, Parks Road, Oxford OX1 3PT.
† To whom correspondence should be addressed.

MS 2070

8. Over short periods, exocytosis may be extremely fast (1 pF/s or 500 granules/s), which is much higher than the rate of endocytosis (18 fF/s or 9 granules/s). Since the latter is in better agreement with the maximum rate of insulin secretion from islets ($\approx$ 2 granules/s), we suggest that membrane retrieval may set an upper limit on the rate of exocytosis during extended periods of secretion.

INTRODUCTION

Changes in the cytoplasmic free calcium concentration ($[Ca^{2+}]_i$) in pancreatic B-cells play an important role in the regulation of insulin secretion. Microelectrode recordings from pancreatic B-cells have demonstrated that glucose stimulation of insulin secretion is associated with the appearance of electrical activity consisting of Ca^{2+}-dependent action potentials (Henquin & Meissner, 1984). The resulting elevation of the cytoplasmic Ca^{2+} concentration ($[Ca^{2+}]_i$) (Santos, Rosario, Nadel, Garcia-Sancho, Soria & Valdeolmillos, 1991; Rorsman, Ämmälä, Berggren, Bokvist & Larsson, 1992; Theler *et al.* 1992) plays a central role in initiating insulin release (reviews: Hellman & Gylfe, 1986; Prentki & Matschinsky, 1987). Indeed, a direct correlation between electrical activity/elevation of $[Ca^{2+}]_i$ and secretion has been demonstrated (Rosario, Atwater & Scott, 1987; Pralong, Bartley & Wollheim, 1990). However, the molecular processes that control the exocytosis of the insulin-containing secretory granules have only been partly elucidated. Earlier studies have been confined principally to measurements of insulin release from islets or suspensions of B-cells (Jones, Fyles & Howell, 1986; Jones, Persaud & Howell, 1989, 1992; Wollheim, Ullrich, Meda & Vallar, 1987), which rarely provide more than one measurement per minute. During the last decade an electrophysiological technique for monitoring exocytosis in single cells with high temporal resolution has been developed by Neher and colleagues (Neher & Marty, 1982; Lindau & Neher, 1988; Joshi & Fernandez, 1988; Fidler Lim, Nowycky & Bookman, 1990). This utilizes the fact that exocytosis involves fusion of the secretory granule with the plasma membrane resulting in an increase in the cell surface area. Since biological membranes have a specific capacitance of about 1 $\mu F/cm^2$ (Hille, 1991), this change can be detected as an increase in the cell capacitance.

In the present study we have combined the patch-clamp technique (Hamill, Marty, Neher, Sakmann & Sigworth, 1981), microfluorimetry and capacitance measurements to record simultaneously whole-cell Ca^{2+} currents, $[Ca^{2+}]_i$ and secretion in individual B-cells. We have used this approach to: (1) explore the temporal relationship between Ca^{2+} influx and the initiation of exocytosis; (2) estimate the $[Ca^{2+}]_i$ dependence of exocytosis; (3) determine the size of the unitary exocytotic events and (4) to study the involvement of Ca^{2+}/calmodulin-dependent protein kinase II in coupling elevation of $[Ca^{2+}]_i$ to activation of the exocytotic machinery.

METHODS

Cells

NMRI mice were purchased from a commercial breeder (Alab, Sollentuna, Sweden). The mice were stunned by a blow against the head and killed by cervical dislocation and decapitation. The pancreas was quickly removed and pancreatic islets isolated by collagenase digestion. Single cells

were prepared as previously described (Rorsman & Trube, 1986). Isolated cells were plated on glass coverslips (diameter: 22 mm) and cultured in RPMI 1640 tissue culture medium supplemented with 5 mM glucose, 10% (v/v) calf serum (Flow Laboratories, Irvine, UK), 100 μg/ml streptomycin and 100 i.u./ml penicillin (both supplied by Northumbria Biologicals Ltd, Cramlington, UK). Coverslips were sealed over a circular hole (diameter: 20 mm) in a stainless-steel plate making a recording chamber in which the coverslip formed the base. The experimental chamber could be perfused and exchange of solution was complete within 1 min. Cells were used within 3 days of isolation.

Electrophysiology

Whole-cell membrane currents were recorded using an EPC-7 patch-clamp amplifier (List Electronic, Darmstadt, FRG). The zero-current potential of the pipette was adjusted with the pipette in the bath and no correction for liquid junction potentials was made. The holding potential was -70 mV. All recordings except those in Figs 12 and 13 were performed using the standard whole-cell configuration. To measure changes in membrane capacitance, a 20 mV r.m.s. 800 Hz sine wave was added to the holding potential (Joshi & Fernandez, 1988; Fidler Lim *et al.* 1990) and ten cycles were averaged for each data point. The resulting current was analysed at two orthogonal phase angles with a resolution of 100 ms per point. The phase angle was determined empirically for each experiment by varying the C_{slow} and G_{series} knobs on the amplifier, normally used to cancel the currents that result from the cell membrane and series conductance of the electrode. We estimate that the small changes in cell conductance that occur during the voltage-clamp depolarizations ($\leqslant 1$ nS) will produce a 0·5 deg change in the phase angle and result in a 0·5% error in the amplitude of the measured capacitance increases. The measurements were performed using a Compaq 386s computer (Houston, TX, USA), a Labmaster AD-DA converter and in-house software written in Axobasic (Axon Instruments, Burlingame, CA, USA). Capacitance changes (reflecting exocytosis) were evoked by interrupting the sinusoidal wave and applying a depolarizing pulse of variable amplitude and duration.

The effects of electrical activity on B-cell exocytosis were assessed by applying action potential waveforms. For this purpose, action potentials were recorded using the perforated patch whole-cell configuration from a B-cell within a cluster which was stimulated with 10 mM glucose. The recorded voltage signal was digitized at 1 kHz (eight and sixteen action potentials) or 4 kHz (one and four action potentials) and stored in the computer. Selected action potential waveforms were then applied to the cell using the D–A converter of the Labmaster board and an Axobasic routine. The voltages were shifted by 10 mV to more depolarized potentials to (partly) compensate for the difference in Ca^{2+} channel gating measured in the standard whole-cell configuration using glutamate-filled electrodes and that observed in perforated patch recordings (10–20 mV; Smith, Ashcroft & Fewtrell, 1993).

Unitary exocytotic events were recorded from cell-attached patches. To increase the likelihood of observing exocytotic events, 2 mM dibutyryl cyclic AMP was added to the extracellular solution. Capacitance was recorded essentially as described for the whole-cell recordings. However, to increase resolution, the frequency of the sine wave was increased to 1600 Hz and 100 cycles were averaged to obtain each data point. The interval between each measurement was ≈ 330 ms. The current, voltage, capacitance and series conductance signals were stored in the computer for later analysis.

Fluorescence measurements

$[Ca^{2+}]_i$ was estimated by dual-emission spectrofluorimetry. We have previously used indo-1 for such measurements (Rorsman *et al.* 1992). In the present experiments we wished to combine the fluorimetric measurements with the use of caged compounds, but the excitation wavelength of indo-1 (360 nm) coincides with that used to liberate the caged compounds. Therefore we have used a combination of the Ca^{2+} indicators fura red (final concentration 34 μM) and fluo-3 (final concentration 6 μM; both indicators from Molecular Probes, Eugene, OR, USA) for all $[Ca^{2+}]_i$ measurements, except those in Figs 7–8 in which indo-1 (0·1 mM) was used. The recordings were made with a Newcastle Photometric System adapted for a Zeiss Axiovert-10 microscope. Excitation was effected at 490 nm by a Zeiss XBO xenon arc lamp. Emitted light was split by a dichroic mirror and detected by two photomultipliers at 525 and 660 nm. Signal processing was performed on-line using a microcomputer (IBM AT clone) and the ratio of the fluorescence detected at 525 and 660 nm (F_{525}/F_{660} ratio) was measured at 10 Hz. Calibration was performed

intracellularly by using the standard whole-cell configuration and dialysing the cell interior with different mixtures of Ca^{2+} and EGTA (calcium calibration buffer kit II; P/N C-3009, Molecular Probes) and the indicators at the above concentrations. Free Ca^{2+} concentration was varied between zero and 39·8 μM. A new cell was used for each measurement and four to six cells tested

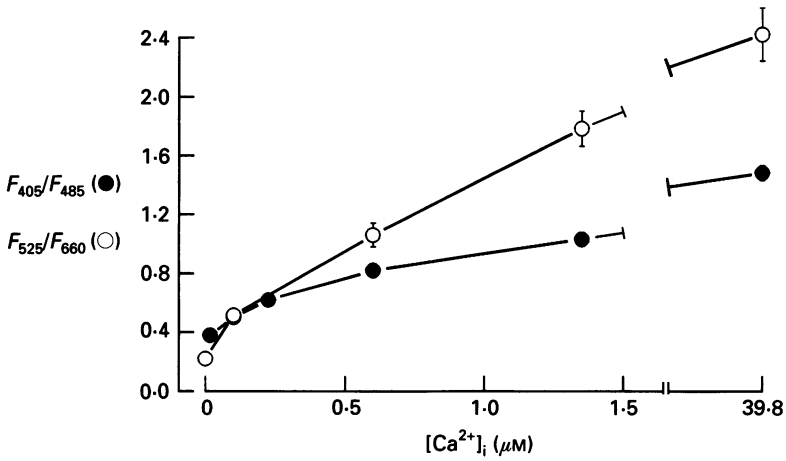

Fig. 1. Calibration curves for indo-1 (●) and fura red/fluo-3 (○) fluorescence ratios. Cells were dialysed with solutions containing from zero to 39·8 μM free Ca^{2+} and with either 100 μM indo-1 or a combination of 34 μM fura red and 6 μM fluo-3. Each data point is the mean ± S.E.M. for four to six different cells.

at each concentration. In all recordings the background values were measured in the cell-attached configuration before establishing the whole-cell conditions. The background amounted to 10–20% of that obtained after equilibration of the indicators. The calibration curve for the combination of fura red/fluo-3 is shown in Fig. 1 and compared with that of the 'conventional' dual-emission indicator indo-1. It can be seen that when $[Ca^{2+}]_i$ is increased from 17 nM to 40 μM the indo-1 fluorescence ratio increases 4-fold whereas there is a > 10-fold increase in the F_{525}/F_{660} ratio when the combination of fluo-3 and fura red was used.

Solutions

The standard extracellular medium consisted of 118 mM NaCl, 20 mM TEA-Cl (to block voltage-activated K^+ currents), 5·6 mM KCl, 1·2 mM $MgCl_2$, 2·6 mM $CaCl_2$, 20 mM glucose and 5 mM Hepes (pH 7·4 with NaOH). For standard whole-cell recordings, the pipette solution contained 125 mM potassium glutamate or caesium glutamate, 10 mM KCl, 10 mM NaCl, 1 mM $MgCl_2$, 3 mM Mg-ATP, 0·1 mM cyclic AMP, 5 mM Hepes (pH 7·15 with KOH or CsOH) and either 0·01 mM EGTA ($[Ca^{2+}]_i$ measurements and Figs 6 and 11), 0·05 mM EGTA (Figs 2 and 3) or 2 mM EGTA (Fig. 4*B*). In one series of experiments, 10 mM EGTA was included in the intracellular solution and 2 or 9 mM $CaCl_2$ added to obtain free Ca^{2+} concentrations of 60 nM and 2 μM, respectively. The Ca^{2+}/calmodulin protein kinase II inhibitors KN-62 and calmodulin-binding domain were both purchased from Calbiochem (San Diego, CA, USA).

For the perforated patch whole-cell recordings (Fig. 13; Horn & Marty, 1988), the pipette solution contained 76 mM Cs_2SO_4, 10 mM NaCl, 10 mM KCl, 1 mM $MgCl_2$ and 5 mM Hepes (pH = 7·35). Electrical contact was established by the addition of amphotericin B (Sigma, St Louis, MO, USA) to the pipette solution. Briefly, a stock solution containing 6 mg of amphotericin dissolved in 100 μl DMSO (dimethyl sulphoxide) was prepared. Twenty microlitres of this stock solution were then added to 5 ml of the pipette solution yielding a final concentration of 0·24 mg/ml. The tip of the pipette was filled with amphotericin-free solution and the pipette was then back-filled with amphotericin solution. Perforation required a few minutes and the voltage clamp regarded as satisfactory when the series conductance was $\geqslant$ 40 nS.

The unitary events (Fig. 12) were recorded in cell-attached patches. The cells were immersed in standard extracellular solution (lacking TEA). The pipette contained extracellular solution

supplemented with 2 mM dibutyryl cyclic AMP and with 20 mM TEA and 0·4 mM tolbutamide to reduce K^+ channel activity in the patch (Trube, Rorsman & Ohno-Shosaku, 1986), and contained 20 mM $CaCl_2$ and 5 μM Bay K8644 to increase Ca^{2+} influx through L-type Ca^{2+} channels (Rorsman, Ashcroft & Trube, 1988).

All recordings were made at 31–34 °C.

Photoliberation of caged inositol 1,4,5-trisphosphate ($InsP_3$)

Intracellular application of $InsP_3$ was achieved by photorelease from 20 μM of the caged precursor (Calbiochem) as previously described (Ämmälä, Bokvist, Galt & Rorsman, 1991). The efficiency of liberation was assumed to be the same as that for caged ATP (70% for 1 s of UV illumination). The break in the $[Ca^{2+}]_i$ record is due to the saturation of the signal by the light flash used to release caged $InsP_3$.

Data analysis

Data are presented as mean values ± S.E.M. and statistical evidence evaluated using Student's *t* test.

RESULTS

Relationship between the length of a voltage-clamp depolarization and the exocytotic response

Figure 2*A* shows the effect of increasing the duration of a depolarizing voltage pulse to 0 mV on the Ca^{2+} current and the associated change in cell capacitance. The mean responses in five different cells are summarized in Fig. 2*B*. Even a depolarization as short as 50 ms is sufficient to elicit a step increase in cell capacitance, which reflects the fusion of secretory granules with the plasma membrane. It is also evident that secretion occurs only during the pulse and ceases immediately upon repolarization. It is not possible to record the capacitance change during the depolarization so that the time course of exocytosis cannot be monitored directly. However, the *mean* rate of the capacitance increase during the depolarization clearly decreased with the pulse duration, from 1·03 ± 0·31 pF/s for a 50 ms pulse to 0·46 ± 0·06 pF/s for a 550 ms pulse. This may explain the tendency to saturation of the capacitance responses for pulses longer than 250 ms (Fig. 2*B*). The gradual decrease in the rate of exocytosis is unlikely to result from exhaustion of the secretory machinery by the preceding pulses as the exocytotic rate measured for the 550 ms depolarization is almost identical to that obtained when a 500 ms depolarization was applied at the beginning of the experiment (0·47 ± 0·10 pF/s; cf. Fig. 10 and related text). In fact, the decrease in the exocytotic rate is not unexpected given that the Ca^{2+} current inactivates which means that the amount of Ca^{2+} entering the cell is not linearly related to the pulse duration (Rorsman *et al.* 1992).

Exocytosis is dependent on influx of calcium and an elevation of $[Ca^{2+}]_i$

Numerous studies have demonstrated the dependence of insulin release on the presence of extracellular Ca^{2+} (review: Hellman & Gylfe, 1986). Figure 3 shows that inclusion of Co^{2+}, a blocker of the Ca^{2+} current in mouse B-cells (Rorsman & Trube, 1986), in the extracellular solution reversibly abolishes both the Ca^{2+} current and the capacitance increase ($n = 4$). In addition to confirming the dependence of exocytosis on Ca^{2+} influx this experiment indicates that depolarization *per se* is not sufficient to initiate exocytosis.

Increasing the intracellular Ca^{2+}-buffering capacity, by inclusion of 2 mM EGTA in the intracellular (pipette) solution, effectively suppresses the ability of the Ca^{2+} current to increase $[Ca^{2+}]_i$ and to initiate exocytosis (Fig. 4). The increase in membrane capacitance evoked by a 500 ms depolarization to 0 mV in cells dialysed

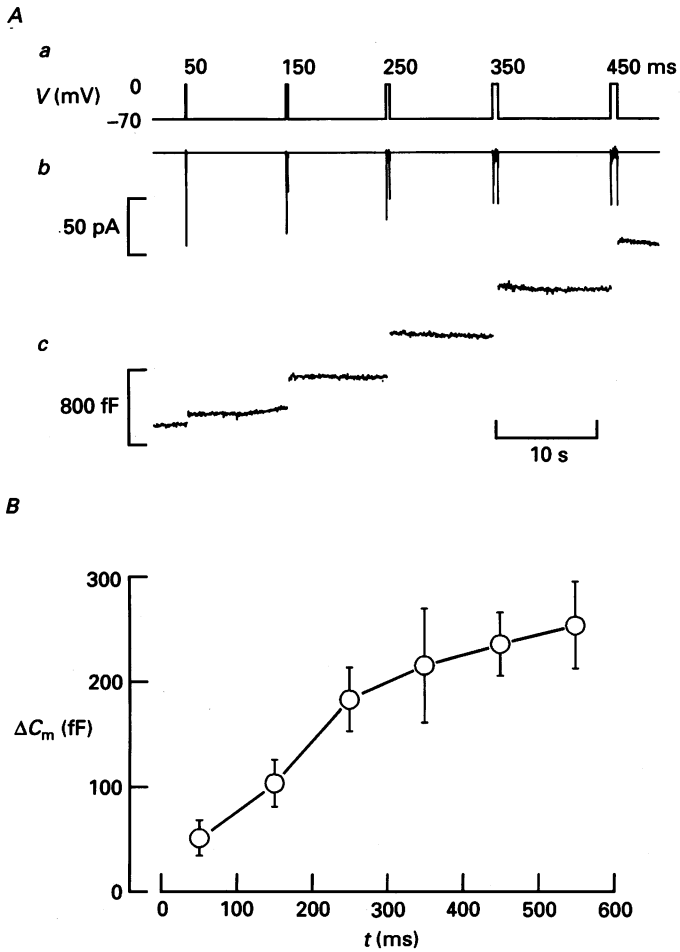

Fig. 2. Relationship between the length of a depolarization and the amplitude of the exocytotic response. *A*, simultaneous recordings of membrane potential (*a*), membrane current (*b*) and cell capacitance (*c*). The duration (ms) of the depolarization to 0 mV from a holding potential of −70 mV is given above the voltage trace. *B*, increase in cell capacitance (ΔC_m) *vs.* duration of depolarization (*t*). Mean values ± S.E.M. of five cells.

with either 10 μM EGTA or 2 mM EGTA averaged 181 ± 27 fF ($n = 16$) and 25 ± 8 fF ($n = 11$; $P < 0{\cdot}001$), respectively. Although inclusion of EGTA in the intracellular solution abolished the ability of a voltage-clamp depolarization to increase $[Ca^{2+}]_i$ and to evoke exocytosis, the inactivation of the Ca^{2+} current, another Ca^{2+}-dependent process (Plant, 1988), was unaffected.

Voltage dependence of capacitance increases

Figure 5*A* shows the relationship between the voltage dependence of the peak Ca^{2+} current, the associated increase in $[Ca^{2+}]_i$ and the change in cell capacitance. The results are summarized in Fig. 5*B*. It is clear that all three processes show the same

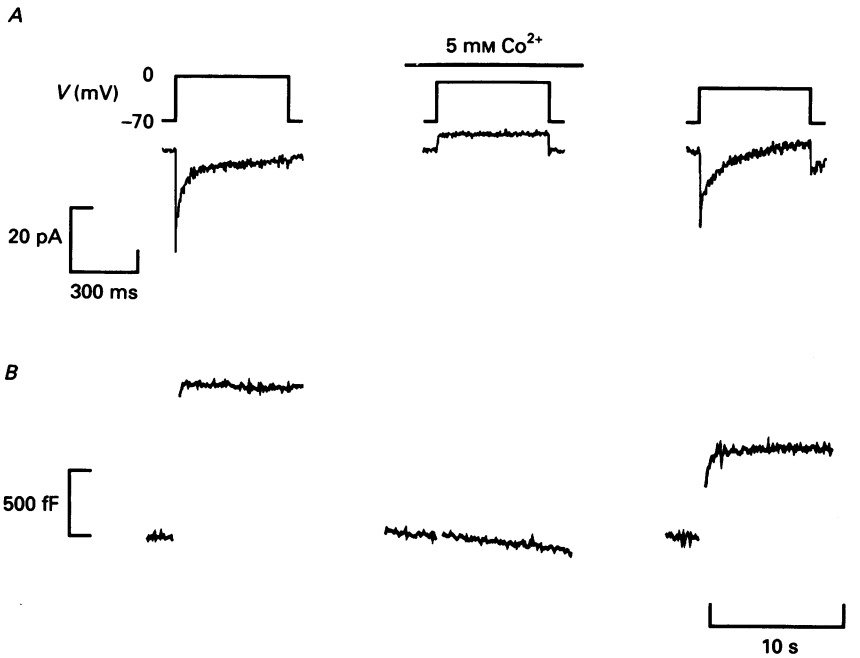

Fig. 3. Exocytosis is dependent on Ca^{2+} influx. *A*, membrane potential (above) and Ca^{2+} currents (below). *B*, capacitance changes associated with the voltage steps in *A*, displayed on a slower time scale. Records shown in the central panel were obtained with extracellular solution supplemented with 5 mM Co^{2+}. The depolarizations went to 0 mV from a holding potential of −70 mV and were applied 60 s apart.

U-shaped voltage dependence with a maximum around +20 mV. A similar voltage dependence of exocytosis has been reported for rat B-cells (Gillis & Misler, 1992). At membrane potentials above +40 mV there is little inward current and correspondingly little change in $[Ca^{2+}]_i$ or cell capacitance. This again excludes the possibility that depolarization *per se* is sufficient to activate exocytosis (cf. Fig. 3). The outward current seen at membrane potentials $\geqslant$ +40 mV probably reflects activation of the delayed rectifying K^+ current, since TEA becomes less efficient as a blocker at positive voltages (Bokvist, Rorsman & Smith, 1990), which obscures the inward Ca^{2+} current. Consequently, it is likely that the inward current is greater than that indicated by the record here. It should be emphasized that the voltage dependence of the Ca^{2+} current recorded with glutamate-filled pipettes is shifted by 30–40 mV to more positive voltages as compared with that observed with Cl^--filled pipettes using the standard whole-cell configuration (Rorsman & Trube, 1986) and by about 20 mV with respect to that found in intact B-cells in perforated-patch whole-cell recordings (Smith, Ashcroft & Fewtrell, 1993). When this shift is taken

into account, the relationship between exocytosis and membrane potential is maximal within the range of the B-cell action potential, which peaks between −20 and 0 mV (Henquin & Meissner, 1984; Ashcroft & Rorsman, 1989).

The relationship between the change in $[Ca^{2+}]_i$ and the associated increase in cell capacitance at various membrane potentials is summarized in Fig. 5*C*. The

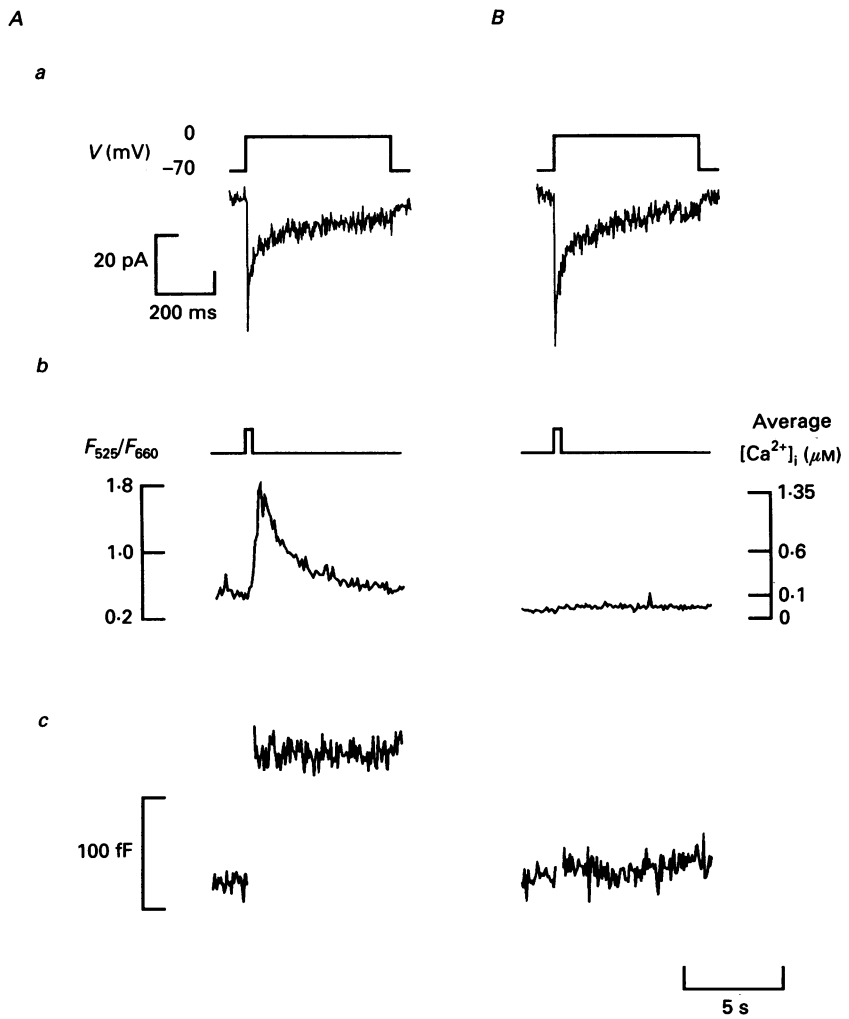

Fig. 4. *A* and *B*, effects of increasing the cytoplasmic Ca^{2+} buffering on Ca^{2+} currents, (*a*, lower), $[Ca^{2+}]_i$ (*b*) and cell capacitance (*c*). The Ca^{2+} currents were evoked by 200 ms depolarizations to 0 mV (*a*, upper). The pipette contained either 10 μM EGTA (*A*) or 2 mM EGTA (*B*). Note that the time base is different for the current and capacitance/$[Ca^{2+}]_i$ traces in both *A* and *B*.

continuous line shows the relationship obtained at voltages of +20 mV and above; i.e. under conditions of maximal Ca^{2+} channel activation (Rorsman & Trube, 1986). It is clear that exocytosis is steeply Ca^{2+} dependent. There was little capacitance

change when the amplitude of the voltage-gated Ca^{2+} transient was $< 0{\cdot}2$ μM. Since the resting $[Ca^{2+}]_i$ measured in fifty-nine cells averaged $0{\cdot}30 \pm 0{\cdot}04$ μM, the threshold for insulin secretion is thus around $0{\cdot}5$ μM $[Ca^{2+}]_i$. The magnitude of the capacitance response increases markedly when $[Ca^{2+}]_i$ exceeds $0{\cdot}4$ μM, that is when $[Ca^{2+}]_i$

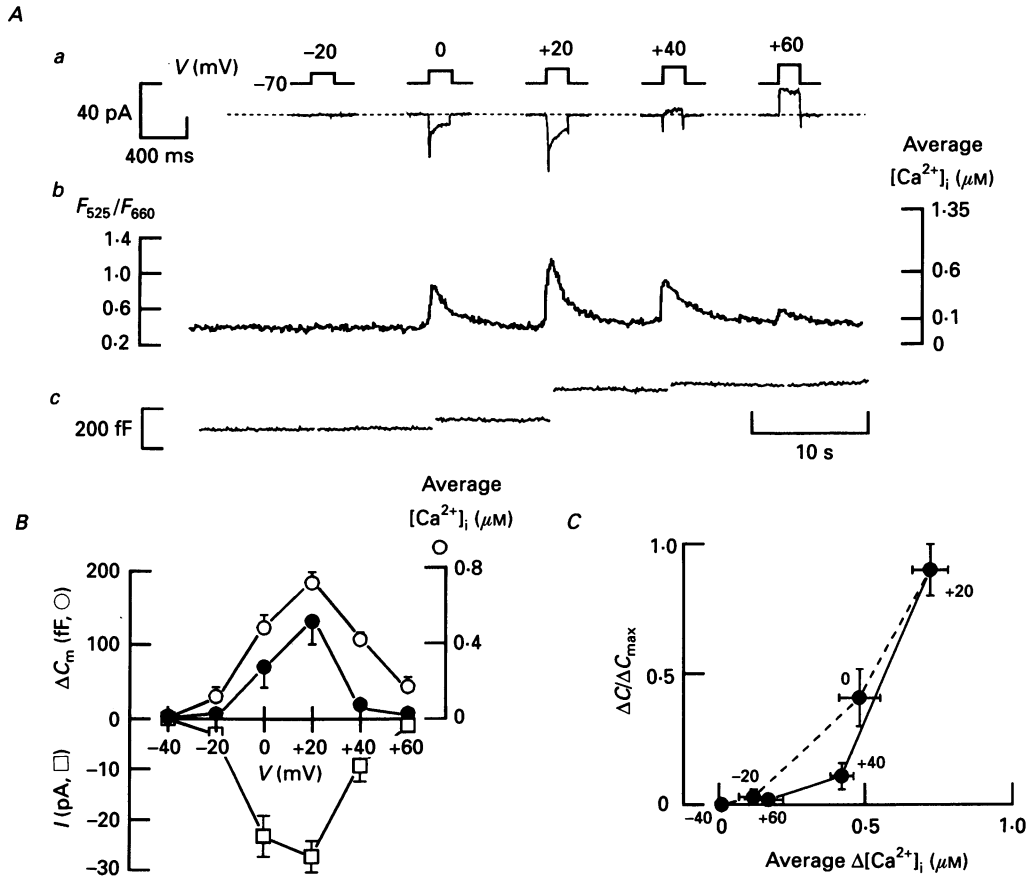

Fig. 5. $[Ca^{2+}]_i$ dependence of exocytosis. *A*, simultaneous recordings of membrane potential (*a*, upper), Ca^{2+} current (*a*, lower), average cytoplasmic free Ca^{2+} concentration ($[Ca^{2+}]_i$) (*b*) and cell capacitance (*c*). The voltage and current records have been displayed on an expanded time base for clarity. 200 ms depolarizations to the potentials indicated (in millivolts) were applied at a frequency of 0·1 Hz. *B*, relationship between the voltage dependence of the change in cell capacitance (ΔC_m, ●; $n = 7$), the magnitude of the $[Ca^{2+}]_i$ transient ($\Delta[Ca^{2+}]_i$, ○; $n = 7$) and the peak inward Ca^{2+} current (□; $n = 7$). *C*, relationship between ΔC_m and $\Delta[Ca^{2+}]_i$ evoked by depolarizations to the indicated potentials. The dashed line connects the responses obtained at -40, -20, 0 and $+20$ mV. The continuous line connects the data points observed following depolarizations to $+20$, $+40$ and $+60$ mV.

approaches $0{\cdot}7$ μM. It is noteworthy that although depolarizations to 0 and $+40$ mV evoke $[Ca^{2+}]_i$ transients of almost identical amplitude, the depolarization to the more negative membrane potential produces significantly more exocytosis ($P < 0{\cdot}05$). This

behaviour was seen irrespective of whether the pulses were applied as shown here or in the reverse order suggesting that it does not result from run-down or depression of exocytosis. The observation that $[Ca^{2+}]_i$ is seemingly more effective as an initiator of exocytosis at negative membrane potentials is in keeping with the domain theory of Ca^{2+} entry as discussed below.

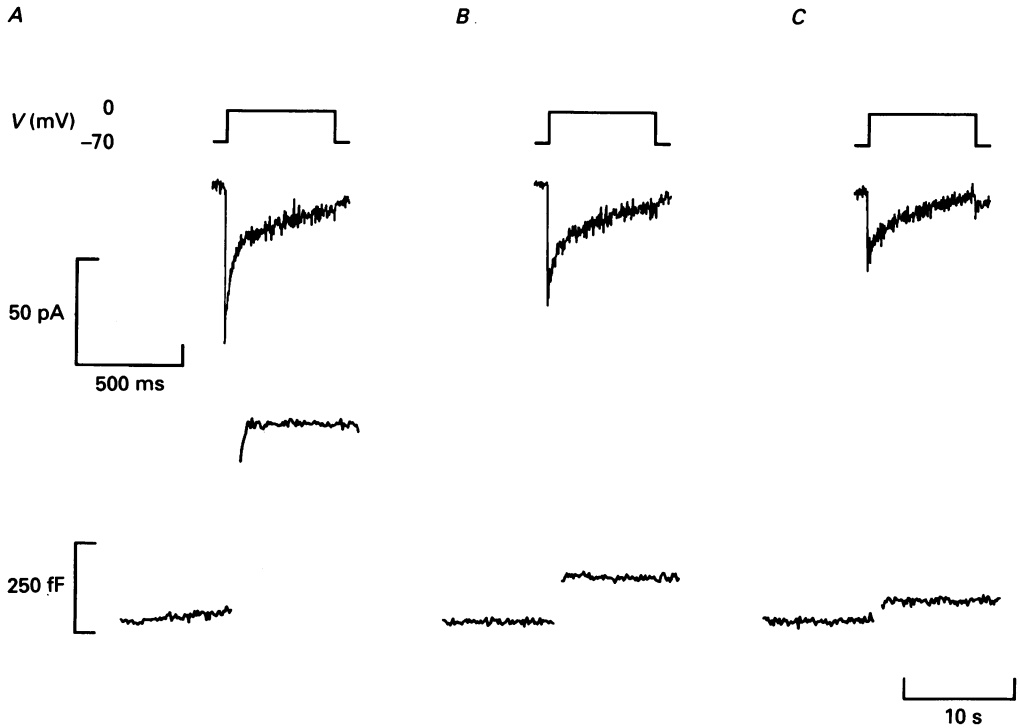

Fig. 6. Run-down of exocytosis. *A–C*, membrane potential (top), Ca^{2+} current (middle) and exocytotic responses (below) observed 3 min (*A*), 5 min (*B*) and 7 min (*C*) after establishment of the whole-cell configuration. The exocytotic responses amounted to 540 fF in *A*, 130 fF in *B* and 60 fF in *C*. The corresponding values for the integrated Ca^{2+} current were 10·2 pC in *A*, 9·7 pC in *B* and 5·2 pC in *C*. Note that the time base is different for the current and capacitance traces.

Rapid run-down of exocytosis during standard whole-cell recordings

During standard whole-cell recordings, the ability of a voltage-clamp depolarization to produce exocytosis declined rapidly following disruption of the patch membrane. A typical experiment is illustrated in Fig. 6 which shows three depolarizations applied at 3, 5 and 7 min after establishment of the whole-cell configuration. Although the integrated Ca^{2+} currents declined during the second and third depolarization, there was a far more dramatic decrease in the exocytotic responses. This suggests that, as previously reported in chromaffin cells (Augustine & Neher, 1992), exocytosis runs down more rapidly than can be accounted for by the decline of the Ca^{2+} current, suggesting some diffusible component necessary for exocytosis is dialysed from the cell. The rapid run-down of exocytosis may be related

to that described for permeabilized B-cells where only the first of a series of pulses of increased intracellular Ca^{2+} is able to stimulate insulin secretion (Jones *et al.* 1992). Run-down of exocytosis is an irreversible process and occurs even when the stimulation frequency is lower than 0·01 Hz.

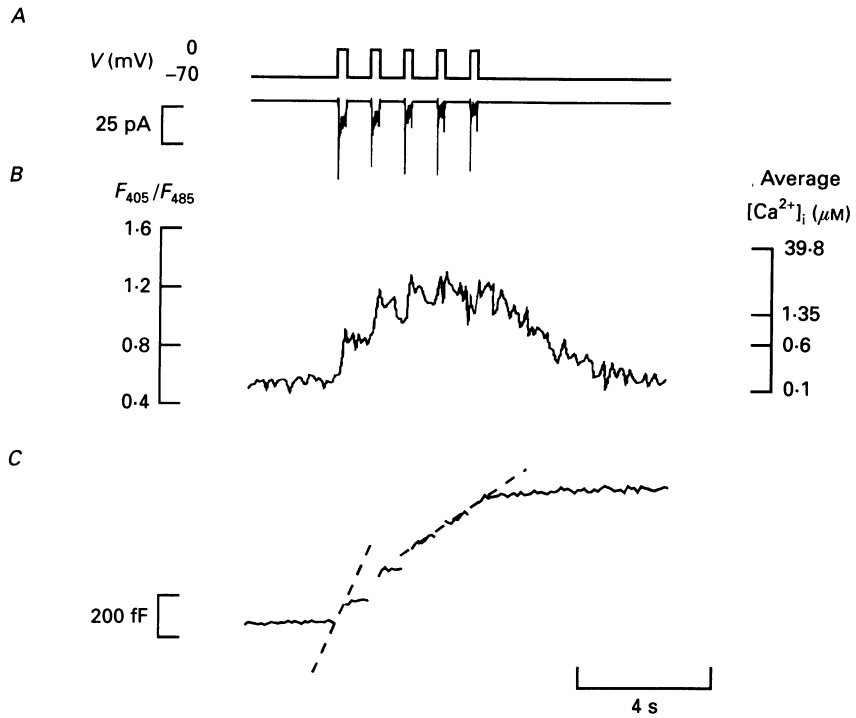

Fig. 7. $[Ca^{2+}]_i$ and exocytosis during repetitive stimulation. Membrane potential (*A*, upper), membrane current (*A*, lower), average $[Ca^{2+}]_i$ (*B*) and cell capacitance (*C*) recorded simultaneously in response to a train of depolarizations consisting of five 200 ms depolarizations to 0 mV (1 Hz stimulation) from a holding potential of −70 mV. Rates of capacitance increase elicited by the first voltage-clamp depolarization and during the interval between the third and fourth pulses are indicated by dashed lines superimposed on the capacitance trace.

Exocytosis during repetitive stimulation

Figure 7*A* shows the Ca^{2+} currents, $[Ca^{2+}]_i$ transients and associated increases in cell capacitance recorded from a B-cell during a train of five 200 ms depolarizations to 0 mV applied at a frequency of 1 Hz. In about 50 % of the cells tested, the largest exocytotic response was observed following the second or third depolarization, reminiscent of the facilitation of neurotransmitter release (or rather the postsynaptic membrane potential changes) documented in neurones (Katz, 1966). This phenomenon is probably the consequence of the failure of $[Ca^{2+}]_i$ to return to basal levels between pulses, resulting in summation of the $[Ca^{2+}]_i$ transients. A similar facilitation of exocytosis has also been reported for other endocrine cells such as pituitary melanotrophs (Thomas, Surprenant & Almers, 1990) and adrenal chromaffin cells

(Augustine & Neher, 1992). In the remaining 50% of B-cells, however, the largest exocytotic response was elicited by the first pulse and subsequent pulses evoked progressively smaller capacitance changes. It is possible that in the latter type of cells, the association between the Ca^{2+} channels and the secretory granules is so close that the first depolarization produces a local $[Ca^{2+}]_i$ increase which is sufficient maximally to activate exocytosis and to deplete a readily releasable pool of granules. Subsequent pulses will consequently produce progressively smaller exocytotic responses, although the measured $[Ca^{2+}]_i$ continues to increase, until finally a depolarization fails to evoke secretion. The latter process which we have called depression (by analogy with a similar process in neurones) should not be confused with the run-down of exocytosis which occurs with a completely different time scale (minutes instead of seconds). Depression is illustrated by the recording in Fig. 8 which shows capacitance increases in a cell subjected to four trains of depolarizations. Whereas exocytosis is elicited by the first depolarization of the first train, no exocytosis occurs in response to the initial pulse of the second train (Fig. 8*B*). This feature becomes even more pronounced during subsequent trains thus giving rise to clearer facilitatory responses. A possible explanation for this observation is that the secretory vesicles located in the close vicinity of the Ca^{2+} channels are released first. Once this pool of vesicles is depleted, Ca^{2+} must diffuse over longer distances to reach releasable secretory granules. It appears therefore, that the process of facilitation may not only reflect accumulation of intracellular Ca^{2+} but also the availability of secretory vesicles in the vicinity of the Ca^{2+} channels.

It is also of interest that although the $[Ca^{2+}]_i$ reported by the indicator remains elevated during the interval between the first and second pulses, exocytosis does not continue after the end of the depolarization and the capacitance trace remains flat during the interpulse interval (Fig. 7). It is only following the third depolarization, when the average $[Ca^{2+}]_i$ attained a value of several micromolar, that continuous exocytosis is observed albeit at a rate lower than that which occurs during depolarization.

Exocytosis evoked by action potentials

The relationship between B-cell electrical activity (simulated action potentials), $[Ca^{2+}]_i$ and exocytosis is examined in Fig. 9*A*. Although a single action potential produced a significant increase in cytosolic Ca^{2+}, it only evoked a small exocytotic response and in two out of five cells tested failed to stimulate exocytosis. The magnitude of both the $[Ca^{2+}]_i$ and capacitance response increased with the number of action potentials and trains of more than four spikes elicited substantial responses in all cells.

The relationship between the increase in $[Ca^{2+}]_i$ and exocytosis produced by varying the number of simulated action potentials is shown in Fig. 9*B*. The $[Ca^{2+}]_i$ dependence of secretion is similar to that measured using voltage-clamp depolarizations (Fig. 5*C*). Thus, secretion is initiated once $[Ca^{2+}]_i$ exceeds $\approx 0{\cdot}5\ \mu M$ and increases steeply with $[Ca^{2+}]_i$.

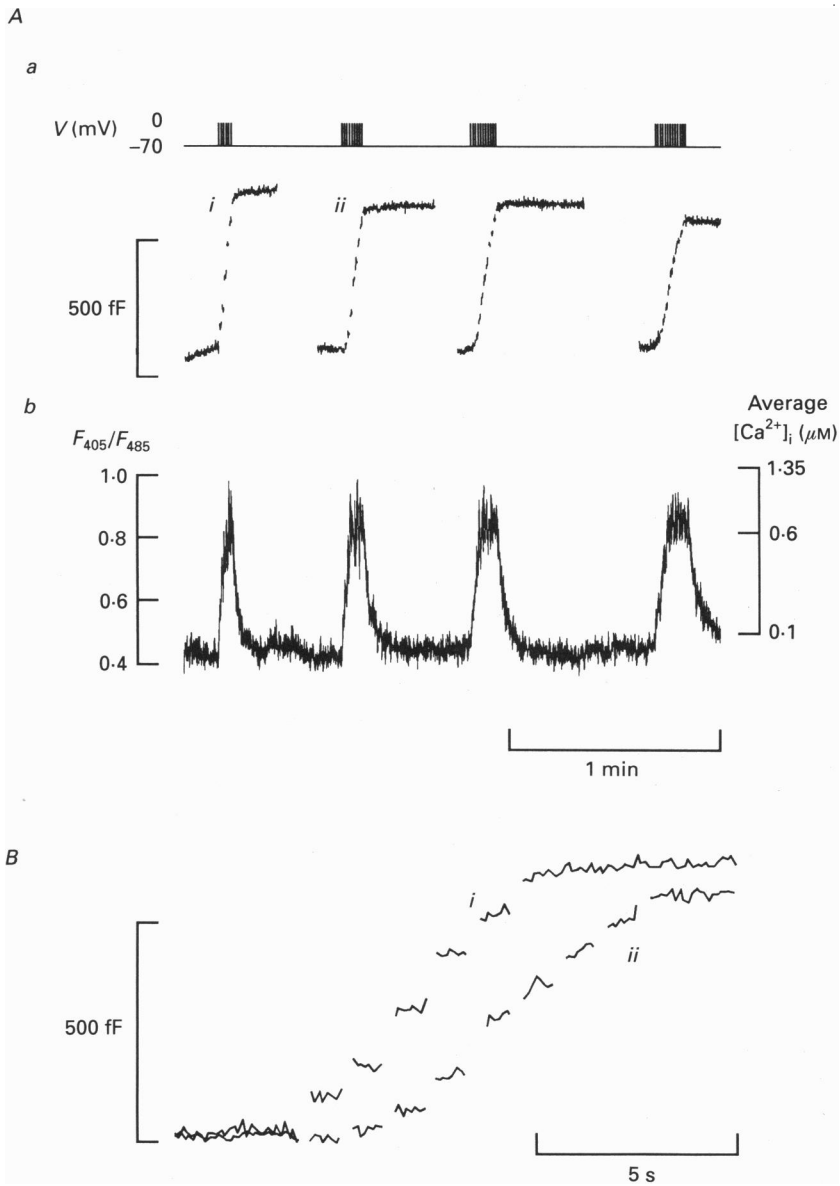

Fig. 8. 'Depression' is not due to run-down. *Aa*, top, four trains of 200 ms depolarizations to 0 mV (pulse frequency: 1 Hz) applied ≈ 30 s apart. *Aa*, below, associated capacitance increases. Parts marked *i* and *ii* are shown on an expanded time base in *B*. Capacitance traces have been reset to the baseline following each train. *Ab*, increases in $[Ca^{2+}]_i$ during pulse trains. *B*, trains *i* and *ii* from *A* shown on an expanded time base. Note that the ability of the first two pulses to evoke exocytosis is dramatically reduced in *ii* but that exocytosis can be evoked by subsequent pulses.

The Ca^{2+} transient evoked by voltage-clamp depolarization is higher at the secretory site than suggested by the fluorescence measurements

In addition to Ca^{2+} influx through voltage-dependent Ca^{2+} channels, $[Ca^{2+}]_i$ may also be elevated by mobilization of Ca^{2+} from intracellular stores (review: Prentki &

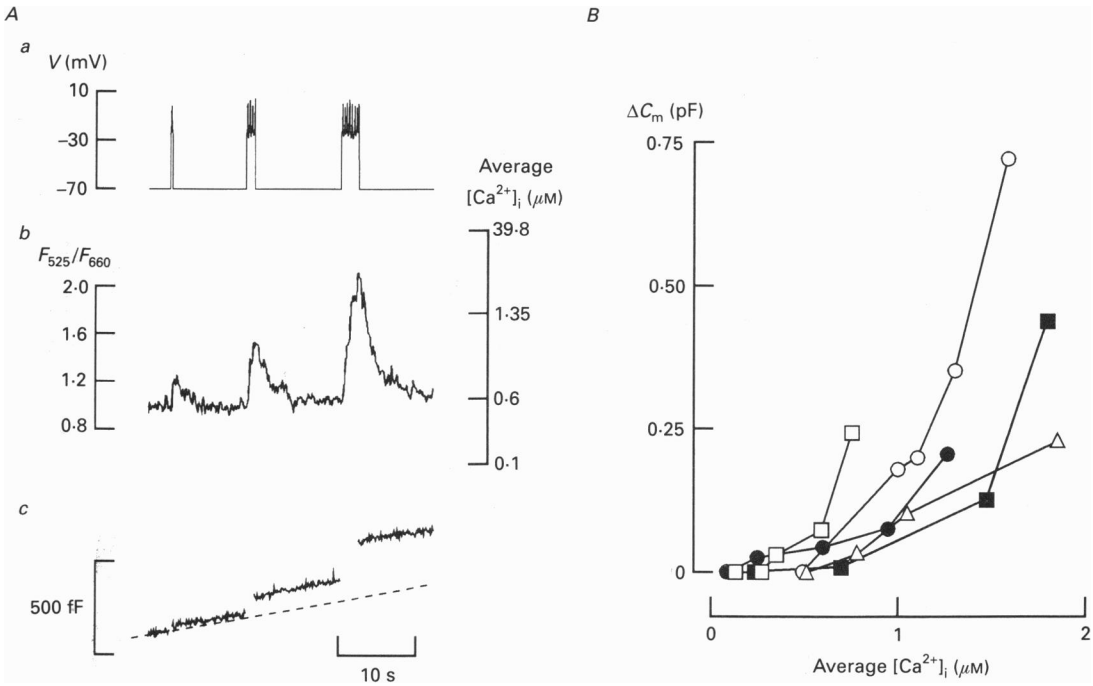

Fig. 9. Electrical activity and exocytosis. *A*, $[Ca^{2+}]_i$ transients (*b*) and cell capacitance changes (*c*) evoked by one, four or eight simulated action potentials (*a*). The dashed line in *c* is drawn through the baseline. *B*, relationship between $[Ca^{2+}]_i$ and the change in cell capacitance (ΔC_m) evoked by one, four, eight or sixteen action potentials measured for the cell shown in *A* (△) and for four other cells (○, □, ■ and ●). The continuous lines connect data points from the same cell. For each experiment, the leftmost point indicates the basal $[Ca^{2+}]_i$ and subsequent points (going from left to right) correspond to the changes in $[Ca^{2+}]_i$ and cell capacitance induced by one, four, eight and sixteen action potentials.

Matschinsky, 1987). Figure 10 compares $[Ca^{2+}]_i$ transients and associated increases in cell capacitance evoked by a 500 ms voltage-clamp depolarization to 0 mV with those produced by intracellular application of $InsP_3$. The voltage-clamp depolarization elicited a $[Ca^{2+}]_i$ transient with an average amplitude of $0{\cdot}56 \pm 0{\cdot}09$ μM and the rate of the capacitance increase averaged $0{\cdot}41 \pm 0{\cdot}09$ pF/s ($n = 12$). Following the recovery of $[Ca^{2+}]_i$ to basal levels, approximately 15 μM of $InsP_3$ was applied by photorelease from a caged precursor. This resulted in a large $[Ca^{2+}]_i$ transient which reached a peak value of 17 ± 7 μM ($n = 12$), considerably larger than that evoked by membrane depolarization ($P < 0{\cdot}05$). Exocytosis initiated by $InsP_3$ was often also of greater absolute magnitude than that which was evoked by depolarization; probably simply because Ca^{2+} is present at stimulatory levels for much longer than following

the voltage-clamp depolarizations. However, the maximum rate of the capacitance increase (measured during the first 0·5–1 s after InsP_3 application) was similar, being $0{\cdot}40 \pm 0{\cdot}08$ pF/s ($n = 12$). The fact that InsP_3 does not evoke a higher rate of exocytosis than a voltage-clamp depolarization, despite a much higher $[Ca^{2+}]_i$, does

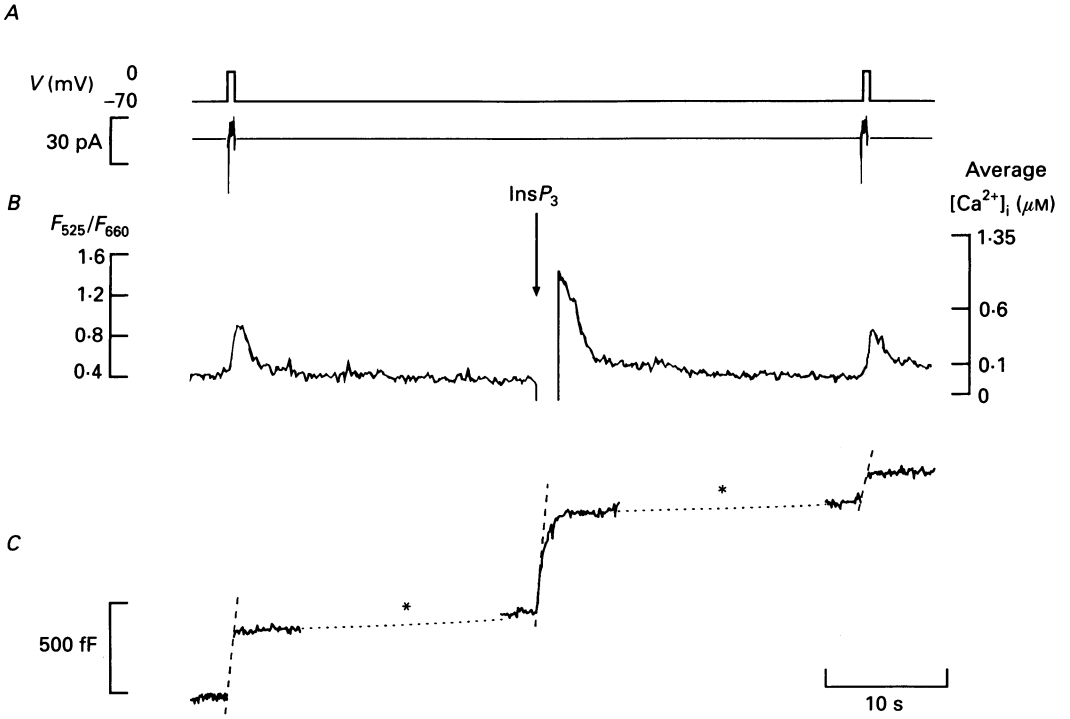

Fig. 10. Comparison of exocytosis evoked by Ca^{2+} entry and by Ca^{2+} release from intracellular stores. Membrane potential (*A*, upper) and whole-cell Ca^{2+} currents (*A*, lower), average cytoplasmic free Ca^{2+} concentration ($[Ca^{2+}]_i$) (*B*) and change in cell capacitance (*C*) recorded using the standard whole-cell configuration. The break in the $[Ca^{2+}]_i$ record is due to saturation of the photomultipliers by the light flash used to release the caged InsP_3. The rates of exocytosis are indicated by the dashed lines superimposed on the capacitance trace. The rate of exocytosis evoked by the first depolarization was 0·76 pF/s. The maximum rate of exocytosis elicited by InsP_3 was 0·56 pF/s (measured during the initial 500 ms) and dropped to 0·12 pF/s during the late phase of exocytosis (measured 1–2 s after InsP_3 release). A voltage-clamp depolarization applied after InsP_3 release evoked a step increase in capacitance corresponding to a rate of 0·31 pF/s. During the periods indicated by the asterisks and dotted lines, the capacitance recordings were interrupted to permit recompensation of C_{slow} and G_{series}.

not imply that the maximum rate of exocytosis is attained at the lower $[Ca^{2+}]_i$ since the maximum rate of exocytosis that can be elicited by a voltage-clamp depolarization (≈ 1 pF/s during a 50 ms pulse; cf. Fig. 2) is in fact twice that observed during a 500 ms depolarization. Also shown in Fig. 10 is that exocytosis stopped within 2 s after application of InsP_3 when $[Ca^{2+}]_i$ reported by the indicator had fallen below 1 μM. It should be emphasized that this is unlikely to result from run-down of the exocytotic capacity as a second depolarization, applied once $[Ca^{2+}]_i$ had returned to basal, remained capable of producing a step capacitance increase.

Exocytosis evoked by adding Ca^{2+} through the recording electrode

When $[Ca^{2+}]_i$ was buffered to 0·06 or 2 μM, by dialysing the cell interior with pipette solutions containing Ca^{2+}–EGTA buffers, the cell capacitance increased gradually after establishment of the whole-cell configuration even when the cell was

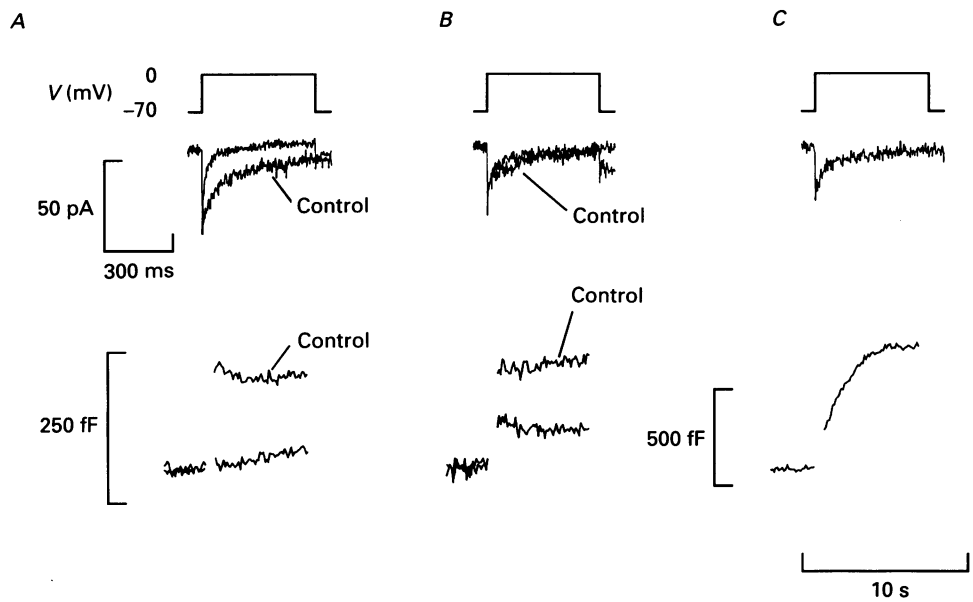

Fig. 11. Ca^{2+}/calmodulin-dependent protein kinase II and regulation of exocytosis. *A*, membrane potential (top), Ca^{2+} current (middle) and cell capacitance (below) recorded with or without (control) pretreatment of the cells for 30 min with 10 μM KN-62. KN-62 was dissolved in DMSO (final concentration of DMSO: 0·1%). Control cells were pretreated with the same concentration of DMSO. *B*, membrane potential (top), Ca^{2+} current (middle) and cell capacitance (below) recorded in the absence (control) or presence of 100 μM calmodulin-binding domain. *C*, membrane potential (top), Ca^{2+} current (middle) and cell capacitance (below) recorded in the presence of 100 μM calmodulin-binding domain. In this and another two cells a slowly developing capacitance increase was observed after the pulse. Note that the time base is different for the current and capacitance traces in *A*, *B* and *C*. In *A* and *B* the records were obtained in different cells. The responses have been superimposed to facilitate comparison.

voltage clamped at −70 mV, a potential which is too negative to permit activation of the voltage-dependent Ca^{2+} channels. At the lower $[Ca^{2+}]_i$, exocytosis was slow as indicated by a low rate of capacitance increase (dC/dt). In six different cells, the average dC/dt was 10 ± 1 fF/s. Increasing $[Ca^{2+}]_i$ to 2 μM recorded resulted in a 7-fold stimulation of exocytosis and the average dC/dt amounted to 75 ± 9 fF/s ($n = 6$; $P < 0{\cdot}001$). Although the latter concentration is considerably higher than that actually observed in response to a depolarization in the microfluorimetric measurements, the observed rate of exocytosis is $< 20\%$ of that recorded during a 200 ms voltage-clamp depolarization to +20 mV (cf. Fig. 5).

Suppression of exocytosis by inhibitors of Ca^{2+}/calmodulin-dependent protein kinase II

Ca^{2+}/calmodulin-dependent protein kinase II (CaM-kinase II) has been shown to play an important role in the regulation of neurotransmitter release (Llinás, Gruner, Sugimori, McGuiness & Greengard, 1991). This kinase has also been identified in B-cells (Harrison & Ashcroft, 1982) but its role in the control of insulin release is not fully understood. As shown in Fig. 11*A*, pretreatment of the B-cells for 30 min with 10 μM KN-62, an inhibitor of CaM-kinase II (Tokumitsu, Chijiwa, Hagiwara, Mizutani, Terasawa & Hidaka, 1990), reduced depolarization-evoked exocytosis by 55% from a control value of 271 ± 51 fF ($n = 12$) to 121 ± 33 fF ($n = 10$; $P < 0{\cdot}025$). The interpretation of these data is complicated, however, by the fact that KN-62 also reduced the peak amplitude of the Ca^{2+} current by 50%, from a control amplitude of 67 ± 11 pA ($n = 12$) to 33 ± 5 pA ($n = 10$; $P < 0{\cdot}025$). The calmodulin-binding domain of CaM-kinase II (residues 290–309) is a potent calmodulin antagonist and a specific inhibitor of CaM-kinase II (Payne *et al.* 1988). As shown in Fig. 11*B*, this antagonist (100 μM) reduced the exocytotic response by 60% when included in the pipette-filling solution, from a control value of 234 ± 52 fF ($n = 9$) to 100 ± 29 fF ($n = 10$; $P < 0{\cdot}05$). This effect was not associated with a decrease in the Ca^{2+} current which amounted to 41 ± 13 pA ($n = 9$) under control conditions and 44 ± 6 pA ($n = 10$) in the presence of the calmodulin-binding domain. Interestingly, in three out of ten cells dialysed with calmodulin-binding domain, the capacitance continued to increase slowly for several seconds after the depolarization (Fig. 11*C*), in contrast to control cells. Pancreatic B-cells are known to contain a high concentration of endogenous calmodulin (15–50 μM; Sugden, Christie & Ashcroft, 1979; Valverde, Vandermeers, Anjaneyulu & Malaisse, 1979) which may be one reason why high concentrations of the calmodulin antagonist were needed to inhibit exocytosis.

Single exocytotic and endocytotic events

We attempted to resolve the small increases in cell capacitance that should result from the fusion of individual secretory granules with the plasma membrane (Neher & Marty, 1982). Figure 12*Aa* shows a recording from a cell-attached patch in which a number of stepwise increases in membrane capacitance (on-steps) can be identified. Although the signal-to-noise ratio is not optimal, these measurements may nevertheless provide an order of magnitude estimate of vesicle size. An idealized trace of this record is presented in Fig. 12*Ab*. The histogram in Fig. 12*B* shows the amplitude distribution of the on-steps, which have a mean amplitude of $1{\cdot}7 \pm 0{\cdot}4$ fF ($n = 31$). Spontaneous decreases in membrane capacitance (off-steps) were also seen (Fig. 12*C*). These had an amplitude distribution similar to that of the on-steps with a mean amplitude of $2{\cdot}1 \pm 0{\cdot}2$ fF ($n = 34$; Fig. 12*D*). Discrete endocytotic steps can be seen in the exocytotic staircase shown in Fig. 12*A*.

The mean values of the on- and off-steps can be used to estimate the size of the secretory granules assuming that their membranes have a specific capacitance of 1 μF/cm^2, which is common for biological membranes (Hille, 1991). This predicts an average diameter of 250 nm, in reasonable agreement with the range of 200–300 nm measured by electron microscopy (Dean, 1973; Hutton, 1989). In Fig. 12*A* and *C*

increases and decreases in membrane capacitance which do not appear as discrete steps are also observable. These may reflect exo- and endocytoses of membrane vesicles too small to be resolved ($< 0{\cdot}5$ fF or < 60 nm in diameter). GABA-containing vesicles of this size have been identified in B-cells (Reetz, Solimena, Matteoli, Folli, Takai & De Camilli, 1991).

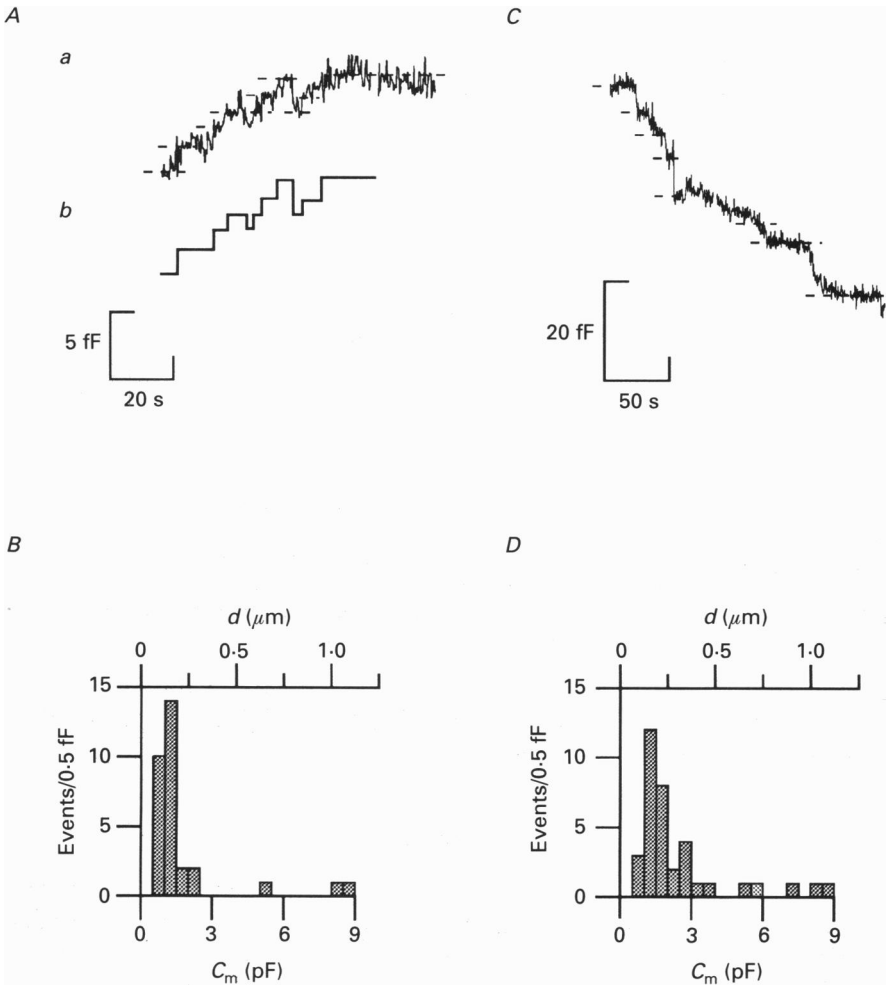

Fig. 12. Single exocytotic and endocytotic events. *Aa*, spontaneous capacitance increases (on-steps). Identified exocytotic events are indicated by the dashed horizontal lines. *Ab*, a possible interpretation of the record is given in the idealized trace of the record shown in *Aa*. *B*, amplitude distribution of the on-steps. *C*, spontaneous capacitance decreases (off-steps). Identified endocytotic events are indicated by the horizontal dashed lines. *D*, amplitude distribution of the endocytotic events. In *B* and *D*, the observed capacitance steps have been converted to expected granule diameter assuming a spherical shape and a specific membrane capacitance of 1 μF/cm^2.

Membrane retrieval was also observed at the whole-cell level but only rarely during standard whole-cell recordings (cf. Figs 2–11). However, when recordings were made from intact B-cells using the perforated-patch whole-cell technique, the

cell capacitance was observed to return to the prestimulatory level following a depolarization-evoked increase in 50% of the cells. We interpret this as endocytosis of the secreted membrane. An example of a cell in which membrane retrieval was unusually rapid is shown in Fig. 13*B* ($\approx$ 100 fF/s). In most cells, however, the

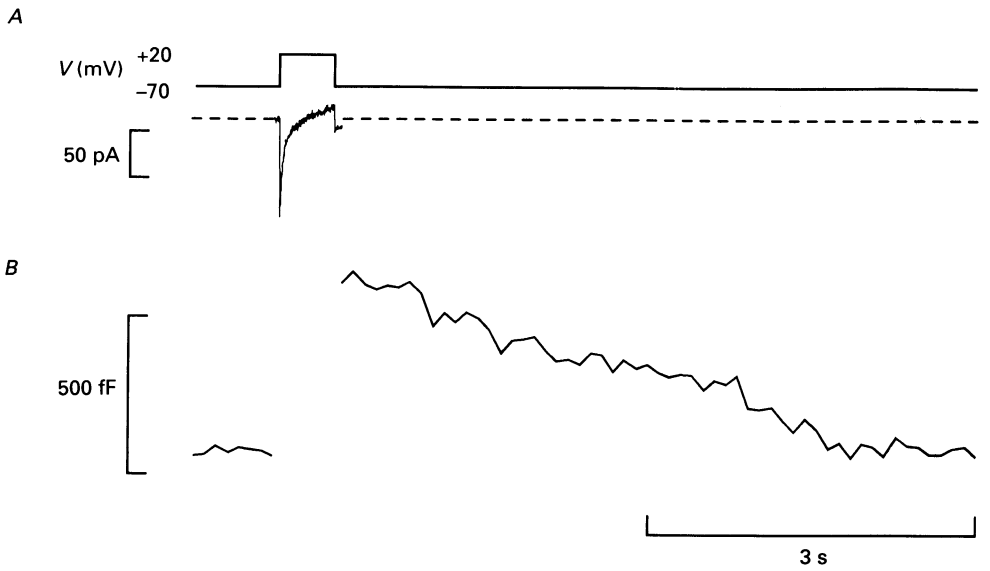

Fig. 13. Endocytosis is slower than exocytosis. *A*, membrane potential (top) and Ca^{2+} current (below). *B*, associated changes in cell capacitance. The records were obtained using the perforated-patch whole-cell configuration. The dashed line indicates the holding current. The extracellular medium was supplemented with 2 μM forskolin.

decline in capacitance was much slower, averaging 18 ± 5 fF/s in fourteen cells; that is $< 2\%$ of the maximal exocytotic rate.

DISCUSSION

We have monitored the secretory activity of single insulin-secreting pancreatic B-cells at a high temporal resolution using capacitance measurements (review: Lindau & Neher, 1988). Our observations are in general agreement with what is known about the release of insulin thus indicating that the capacitance measurements do indeed reflect the exocytosis of the insulin-containing secretory granules. In this study we have concentrated on the action of Ca^{2+} as an initiator and regulator of insulin secretion. It should be emphasized, however, that in the intact B-cells factors other than, or in addition to, Ca^{2+} are likely to participate in the regulation of exocytosis.

Ca^{2+} is high at the secretory site

Several lines of argument suggest that during depolarization-evoked exocytosis, the secretory machinery is regulated by the $[Ca^{2+}]_i$ level beneath the plasma membrane and that in the B-cell, as in neurones (Sala & Hernández-Cruz, 1990; Llinás, Sugimori & Silver, 1992), steep spatial gradients of Ca^{2+} exist.

First, the observation that similar rates of exocytosis were induced by a voltage-clamp depolarization and by InsP_3-evoked Ca^{2+} release, despite markedly different *average* $[Ca^{2+}]_i$ levels (Fig. 10), is easiest to explain by assuming that when Ca^{2+} channels are opened by depolarization, $[Ca^{2+}]_i$ in the vicinity of the secretory granules rises to concentrations considerably higher than that reported by the fluorescent indicator.

Second, exocytosis usually does not continue following membrane repolarization despite an elevated $[Ca^{2+}]_i$. This suggests that the $[Ca^{2+}]_i$ transient sensed by the secretory granules rapidly decreases on repolarization. Likewise, we observed that during repetitive stimulation (Fig. 7) exocytosis did not proceed during the first two interpulse intervals, although the measured $[Ca^{2+}]_i$ remained high. It was only following the third depolarization, when the average $[Ca^{2+}]_i$ attained a plateau concentration of several micromolar, that exocytosis continued after the pulse. However, the rate was still lower than that which occurred during the preceding depolarization. These results can be explained by assuming that a locally high $[Ca^{2+}]_i$ adjacent to the release sites rapidly collapses following closure of the Ca^{2+} channels. Since only a small fraction of the dye is located at the exocytotic release site, the fluorescence measurements underestimate the actual Ca^{2+} concentration at the release site during the two first two depolarizations. This may be because the time needed for Ca^{2+} to diffuse away from the release sites is much shorter than the time constant for the removal of Ca^{2+} from the cytoplasm (1 s; Rorsman *et al.* 1992). Therefore Ca^{2+} accumulates in the cytosol during repetitive stimulation until eventually the average $[Ca^{2+}]_i$ reported by the indicator approaches the true concentration at the secretory sites (Sala & Hernández-Cruz, 1990; Augustine & Neher, 1992; Neher & Augustine, 1992).

Third, even when the B-cell was dialysed with a solution containing 2 μM free Ca^{2+}, which is about twice that measured during a 200 ms depolarization to +20 mV (Fig. 5), the rate of exocytosis (measured as dC/dt; cf. Augustine & Neher, 1992) was less than 20 % of that observed during the voltage-clamp pulse. This is again easiest to explain assuming that $[Ca^{2+}]_i$ in the close vicinity of the Ca^{2+} channels rises to concentrations much higher than those reported by the indicators.

Fourth, the observation that larger exocytotic responses were observed at 0 mV than at +40 mV, although the measured $[Ca^{2+}]_i$ was the same, supports the idea that it is the local $[Ca^{2+}]_i$ just beneath the plasma membrane that determines the rate of exocytosis. The domain hypothesis of Ca^{2+} entry (Chad & Eckert, 1984) predicts that, because of the inwardly rectifying properties of the Ca^{2+} channel, the local $[Ca^{2+}]_i$ transients close to the Ca^{2+} channel will be larger (and thus more effective at initiating exocytosis) at the more negative membrane potential. A similar relationship between the Ca^{2+} currents, $[Ca^{2+}]_i$ transients and exocytosis has recently been reported in chromaffin cells (Augustine & Neher, 1992).

It appears, however, that *some* diffusion of Ca^{2+} is necessary to initiate exocytosis because of the different effects of intracellular EGTA on exocytosis and Ca^{2+} current inactivation. The latter is also regulated by $[Ca^{2+}]_i$ in the vicinity of the Ca^{2+} channel (Plant, 1988) but unlike exocytosis inactivation of the Ca^{2+} current was not affected by EGTA. The failure of EGTA to reduce Ca^{2+} current inactivation can be explained by the slow binding kinetics of the chelator which means that during Ca^{2+} channel

openings $[Ca^{2+}]_i$ rises too rapidly to be buffered. A similar argument has previously been used to account for the resistance of neurotransmitter release to EGTA (Adler, Augustine, Duffy & Charlton, 1991). These considerations suggest that in order to evoke exocytosis in the B-cell, Ca^{2+} must act over a longer distance than that required to produce Ca^{2+}-channel inactivation or neurotransmitter release from neurones. This allows Ca^{2+} buffering by EGTA to occur. It seems possible that the differences in the EGTA sensitivity of neurotransmitter release and of exocytosis from B-cells and chromaffin cells (Neher & Marty, 1982) may simply reflect the fact that the hormone-containing vesicles are 5–10 times larger than the synaptic vesicles (diameter 200–300 *vs.* 40 nm).

The rate of exocytosis in the B-cell is larger than suggested by biochemical measurements

Comparison of the capacitance increase due to a single exocytotic event (2 fF) with the observed whole-cell capacitance changes (400–1000 fF/s) indicates that exocytosis may occur at rates of up to 500–600 secretory granules per second. In a B-cell with an average of 13000 secretory granules (Dean, 1973), this corresponds to 4–5% of the total granule population per second. This release rate is far greater than that suggested by previous biochemical experiments (Jones *et al.* 1989) and indicates that the exocytotic machinery of the B-cell is capable of operating at very high rates. It must be emphasized, however, that such a high rate of exocytosis is unlikely to occur except for short periods and that during repetitive stimulation the exocytotic responses usually decrease with time until eventually depolarization fails to produce a capacitance increase (Figs 7 and 8 and Gillis & Misler, 1992). It seems likely that *in vivo* the rate of exocytosis must be balanced by the rate of membrane retrieval. The latter would consequently be expected to set a limit on the rate of exocytosis over long time periods. It is interesting therefore that the rate of retrieval (18 fF/s or 4% of the total granule number per minute) corresponds more closely to that seen for insulin release in biochemical measurements (< 1–5%/min; Jones *et al.* 1989; Li, Hidaka & Wollheim, 1992; Bergsten & Hellman, 1992).

Initiation of exocytosis requires bursts of action potentials

Our data suggest that the amount of exocytosis that can be evoked by a single action potential is quite small. Indeed, because of the steep $[Ca^{2+}]_i$ dependence and the facilitation of exocytosis, groups of action potentials will be more effective at initiating exocytosis than the same number of single action potentials fired at a frequency too low (< 1 Hz) to permit the individual $[Ca^{2+}]_i$ transients to summate. This may provide a functional explanation for the characteristic pattern of B-cell electrical activity, which, over the range of glucose concentrations which stimulate release physiologically, consists of bursts of action potentials (Henquin & Meissner, 1984; Ashcroft & Rorsman, 1989).

Ca^{2+}/calmodulin-dependent protein kinase II and exocytosis in the B-cell

The activation of intracellular protein kinases is believed to be an important step in the initiation of exocytosis (review: Ashcroft & Ashcroft, 1992). Elevation of the cytosolic Ca^{2+} concentration in B-cells produces rapid phosphorylation of a protein

with a molecular mass of 53–54 kDa (Harrison & Ashcroft, 1982; Jones *et al.* 1992). This Ca^{2+}-dependent phosphorylation requires the presence of calmodulin and is blocked by calmodulin antagonists. It has therefore been proposed that the phosphorylation reflects the activity of a Ca^{2+}/calmodulin-dependent protein kinase. Indeed, CaM-kinase II has been identified in B-cells (Harrison & Ashcroft, 1982). Evidence for a role for CaM-kinase II in regulating insulin secretion is provided by the observation that inhibitors of this kinase reduce nutrient-stimulated insulin secretion and block the potentiating effects of forskolin (Harrison, Poje, Rocic & Ashcroft, 1986; Li *et al.* 1992). Since the CaM-kinase II inhibitor KN-62 blocked Ca^{2+} influx but did not affect Ca^{2+}-induced insulin secretion from permeabilized cells it was argued that CaM-kinase II does not regulate the secretory machinery itself (Li *et al.* 1992). However, our observation that calmodulin-binding domain reduces exocytosis without affecting Ca^{2+} currents suggests that CaM-kinase II regulates exocytosis distal to the elevation of $[Ca^{2+}]_i$, probably by phosphorylating proteins involved in the release process. The identity of the substrate(s) phosphorylated by the kinase has not been established. It has been proposed that one substrate may be a subunit of tubulin (Colca, Wolf, Comens & McDaniel, 1983) and is thus involved in regulating the interactions between the cytoskeleton and the secretory granules. This is reminiscent of the situation in neurones where phosphorylation of the synaptic vesicle-associated protein synapsin I by CaM-kinase II leads to the dissociation of the synaptic vesicles from the cytoskeleton thus facilitating their translocation to and fusion with the plasma membrane (Llinàs *et al.* 1991). However, the synapsins are known to be neurone specific and there is no evidence for their presence in the pancreatic B-cells. Nevertheless it is tempting to speculate that a protein functionally (but not necessarily structurally) related to the synapsins participates in the control of exocytosis of the insulin-containing secretory granules.

Financial support was obtained from the Åke Wibergs Stiftelse, the Swedish Medical Research Council (12X-08647), the Swedish Diabetes Association, the Nordic Insulin Foundation Committee, the Swedish Hoechst, the O.E. och Edla Johanssons vetenskapliga stiftelse, the Swedish Society for Medicine, the Svenska Sällskapet för medicinsk forskning and the Royal Swedish Academy of Sciences. F.M.A.'s visits to Gothenburg were made possible by grants from the Wellcome Trust and the British Medical Research Council.

REFERENCES

ADLER, E. M., AUGUSTINE, G. J., DUFFY, S. N. & CHARLTON, M. P. (1991). Alien intracellular calcium chelators attenuate neurotransmitter release at the squid giant synapse. *Journal of Neuroscience* **11**, 1496–1507.

ÄMMÄLÄ, C., BOKVIST, K., GALT, S. & RORSMAN, P. (1991). Inhibition of ATP-regulated K^+-channel by a photoactivatable ATP-analogue in mouse pancreatic β-cells. *Biochimica et Biophysica Acta* **1092**, 347–349.

ASHCROFT, F. M. & ASHCROFT, S. J. H. (1992). Mechanisms of insulin secretion. In *Insulin: Molecular Biology to Pathology*, ed. ASHCROFT, F. M. & ASHCROFT, S. J. H., pp. 97–150. IRL Press, Oxford.

ASHCROFT, F. M. & RORSMAN, P. (1989). Electrophysiology of the pancreatic β-cell. *Progress in Biophysics and Molecular Biology* **54**, 87–143.

AUGUSTINE, G. J. & NEHER, E. (1992). Calcium requirements for secretion in bovine chromaffin cells. *Journal of Physiology* **450**, 247–271.

BERGSTEN, P. & HELLMAN, P. (1992). The individual islet responds to glucose with amplitude modulation of rapid insulin transients. *Diabetologia* **35**, A110.

BOKVIST, K., RORSMAN, P. & SMITH, P. A. (1990). Effects of external tetraethylammonium ions and quinine on delayed rectifying K^+-channels in mouse pancreatic β-cells. *Journal of Physiology* **423**, 311–325.

CHAD, J. E. & ECKERT, R. (1984). Calcium domains associated with individual channels can account for anomalous relations of Ca-dependent responses. *Biophysical Journal* **45**, 993–999.

COLCA, J. R., WOLF, B. A., COMENS, P. G. & MCDANIEL, M. L. (1983). Correlation of Ca^{2+}- and calmodulin-dependent protein kinase activity with secretion of insulin from islets of Langerhans. *Biochemical Journal* **212**, 819–827.

DEAN, P. M. (1973). Ultrastructural morphometry of the pancreatic beta-cell. *Diabetologia* **9**, 115–119.

FIDLER LIM, N., NOWYCKY, M. C. & BOOKMAN, R. J. (1990). Direct measurements of exocytosis and calcium currents in single vertebrate nerve terminals. *Nature* **344**, 449–451.

GILLIS, K. D. & MISLER, S. (1992). Single cell assay of exocytosis from pancreatic islet B cells. *Pflügers Archiv* **420**, 121–123.

HAMILL, O. P., MARTY, A., NEHER, E., SAKMANN, B. & SIGWORTH, F. J. (1981). Improved patch-clamp techniques for high-resolution recording from cells and cell-free membrane patches. *Pflügers Archiv* **391**, 85–100.

HARRISON, D. E. & ASHCROFT, S. J. H. (1982). Effects of Ca^{2+}, calmodulin and cyclic AMP on the phosphorylation of endogenous proteins by homogenates of rat islets of Langerhans. *Biochimica et Biophysica Acta* **714**, 313–319.

HARRISON, D. E., POJE, M., ROCIC, B. & ASHCROFT, S. J. H. (1986). Effects of dihydrouramil on protein phosphorylation and insulin secretion in rat islets of Langerhans. *Biochemical Journal* **237**, 191–196.

HELLMAN, B. & GYLFE, E. (1986). Calcium and the control of insulin secretion. In *Calcium and Cell Function*, vol. VI, ed. CHEUNG, W. Y., pp. 253–326. Academic Press, Orlando, FL, USA.

HENQUIN, J. C. & MEISSNER, H. P. (1984). Significance of ionic fluxes and changes in membrane potential for stimulus–secretion coupling in pancreatic B-cells. *Experientia* **40**, 1043–1052.

HILLE, B. (1991). *Ionic Channels of Excitable Membranes*, pp. 9–11. Sinauer, Sunderland, MA, USA.

HORN, R. & MARTY, A. (1988). Muscarinic activation of ionic currents measured by a new whole-cell recording method. *Journal of General Physiology* **92**, 145–159.

HUTTON, J. C. (1989). The insulin secretory granule. *Diabetologia* **32**, 271–281.

JONES, P. M., FYLES, J. M. & HOWELL, S. L. (1986). Regulation of insulin secretion by cAMP in rat islets of Langerhans. *FEBS Letters* **205**, 205–209.

JONES, P. M., PERSAUD, S. J. & HOWELL, S. L. (1989). Time course of Ca^{2+}-induced insulin secretion from perifused, electrically permeabilised islets of Langerhans: effects of cAMP and a phorbol ester. *Biochemical and Biophysical Research Communications* **162**, 998–1003.

JONES, P. M., PERSAUD, S. J. & HOWELL, S. L. (1992). Ca^{2+}-induced insulin secretion from electrically permeabilized cells. Loss of the Ca^{2+}-induced secretory response is accompanied by loss of Ca^{2+}-induced protein phosphorylation. *Biochemical Journal* **285**, 973–978.

JOSHI, C. & FERNANDEZ, J. (1988). Capacitance measurements. An analysis of the phase detector technique used to study exocytosis and endocytosis. *Biophysical Journal* **53**, 885–892.

KATZ, B. (1966). *Nerve, Muscle and Synapse*, pp. 139–141. McGraw-Hill, New York.

LI, G., HIDAKA, H. & WOLLHEIM, C. B. (1992). Inhibition of voltage-gated Ca^{2+} channels and insulin secretion in HIT cells by the Ca^{2+}/calmodulin-dependent protein kinase II inhibitor KN-62. Comparison with antagonists of calmodulin and L-type Ca^{2+} channels. *Molecular Pharmacology* **42**, 489–498.

LINDAU, M. & NEHER, E. (1988). Patch-clamp techniques for time-resolved capacitance measurements in single cells. *Pflügers Archiv* **411**, 137–146.

LLINÁS, R., GRUNER, J. A., SUGIMORI, M., MCGUINNESS, T. L. & GREENGARD, P. (1991). Regulation by synapsin I and Ca^{2+}-calmodulin-dependent protein kinase II of the transmitter release in squid giant synapse. *Journal of Physiology* **436**, 257–282.

LLINÁS, R., SUGIMORI, M. & SILVER, R. B. (1992). Microdomains of high calcium concentration in a presynaptic terminal. *Science* **256**, 677–679.

NEHER, E. & AUGUSTINE, G. J. (1992). Calcium gradients and buffers in bovine chromaffin cells. *Journal of Physiology* **450**, 273–301.

NEHER, E. & MARTY, A. (1982). Discrete changes of cell membrane capacitance observed under conditions of enhanced secretion in bovine adrenal chromaffin cells. *Proceedings of the National Academy of Sciences of the USA* **79**, 6712–6716.

PAYNE, E. M., FONG, Y. L., ONO, T., COLBRAN, R. J., KEMP, B. E., SODERLING, T. R. & MEANS, A. R. (1988). Calcium/calmodulin-dependent protein kinase II. Characterization of distinct calmodulin binding and inhibitory domains. *Journal of Biological Chemistry* **263**, 7190–7195.

PLANT, T. D. (1988). Properties of calcium-dependent inactivation of calcium currents in cultured mouse pancreatic B-cells. *Journal of Physiology* **404**, 731–747.

PRALONG, W. F., BARTLEY, C. & WOLLHEIM, C. B. (1990). Single islet β-cell stimulation by nutrients: relationship between pyridine nucleotides, cytosolic Ca^{2+} and secretion. *EMBO Journal* **9**, 53–60.

PRENTKI, M. & MATSCHINSKY, F. M. (1987). Ca^{2+}, cAMP and phospholipid-derived messengers in coupling mechanisms of insulin secretion. *Physiological Reviews* **67**, 1185–1249.

REETZ, A., SOLIMENA, M., MATTEOLI, M., FOLLI, F., TAKAI, K. & DE CAMILLI, P. (1991). GABA and pancreatic β-cells: colocalization of glutamic acid decarboxylase (GAD) and GABA with synaptic-like microvesicles suggests their role in GABA storage and secretion. *EMBO Journal* **10**, 1275–1284.

RORSMAN, P., ÄMMÄLÄ, C., BERGGREN, P.-O., BOKVIST, K. & LARSSON, O. (1992). Cytoplasmic calcium transients due to single action potentials and voltage-clamp depolarizations in mouse pancreatic B-cells. *EMBO Journal* **11**, 2877–2884.

RORSMAN, P., ASHCROFT, F. M. & TRUBE, G. (1988). Single Ca channel currents in mouse pancreatic B-cells. *Pflügers Archiv* **412**, 597–603.

RORSMAN, P. & TRUBE, G. (1986). Calcium and delayed potassium currents in mouse pancreatic β-cells under voltage-clamp conditions. *Journal of Physiology* **374**, 531–550.

ROSARIO, L. M., ATWATER, I. & SCOTT, A. M. (1987). Pulsatile insulin release and electrical activity from single ob/ob mouse islets of Langerhans. *Advances in Experimental Medicine and Biology* **211**, 413–425.

SALA, F. & HERNÁNDEZ-CRUZ, A. (1990). Calcium diffusion modeling in a spherical neuron. Relevance of buffering properties. *Biophysical Journal* **57**, 313–324.

SANTOS, R. M., ROSARIO, L. M., NADEL, A., GARCIA-SANCHO, J., SORIA, B. & VALDEOLMILLOS, M. (1991). Widespread synchronous $[Ca^{2+}]_i$ oscillations due to bursting electrical activity in single pancreatic islets. *Pflügers Archiv* **418**, 417–422.

SMITH, P. A., ASHCROFT, F. M. & FEWTRELL, C. M. S. (1993). Permeation and gating properties of the L-type calcium channel in mouse pancreatic β-cells. *Journal of General Physiology* **101**, 767–797.

SUGDEN, M. C., CHRISTIE, M. R. & ASHCROFT, S. J. H. (1979). Protein kinase activities in rat pancreatic islets of Langerhans. *FEBS Letters* **105**, 95–100.

THELER, J. M., MOLLARD, P., GUÉRINEAU, N., VACHER, P., PRALONG, W. F., SCHLEGEL, W. & WOLLHEIM, C. B. (1992). Video imaging of cytosolic Ca^{2+} in pancreatic β-cells stimulated by glucose, carbachol, and ATP. *Journal of Biological Chemistry* **267**, 18110–18117.

THOMAS, P., SURPRENANT, A. & ALMERS, W. (1990). Cytosolic Ca^{2+}, exocytosis and endocytosis in single melanotrophs of the rat pituitary. *Neuron* **5**, 723–733.

TOKUMITSU, H., CHIJIWA, T., HAGIWARA, M., MIZUTANI, A., TERASAWA, M. & HIDAKA, H. (1990). KN-62, 1-[*N*,*O*-bis(5-isoquinolinesulfonyl)-*N*-methyl-L-tyrosyl]-4-phenyl-piperazine, a specific inhibitor of Ca^{2+}/calmodulin-dependent protein kinase II. *Journal of Biological Chemistry* **265**, 4315–4320.

TRUBE, G., RORSMAN, P. & OHNO-SHOSAKU, T. (1986). Opposite effects of tolbutamide and diazoxide on the ATP-dependent K^+ channel in mouse pancreatic β-cells. *Pflügers Archiv* **407**, 493–499.

VALVERDE, I., VANDERMEERS, A., ANJANEYULU, R. & MALAISSE, W. J. (1979). Calmodulin activation of adenylate cyclase in pancreatic islets. *Science* **206**, 225–227.

WOLLHEIM, C. B., ULLRICH, S., MEDA, P. & VALLAR, L. (1987). Regulation of exocytosis in electrically permeabilized insulin-secreting cells. Evidence for Ca^{2+} dependent and independent secretion. *Bioscience Reports* **7**, 443–454.